

Study of the Influence of Additions on the Formation of Microstructure of Al-Zn-Mg-Cu Alloys

B.P. Pisarek ^{a,*}, E. Czekaj ^b, T. Pacyniak ^a

^a Department of Materials Engineering and Production Systems of Lodz University of Technology, Stefanowskiego 1/15, 90-924 Łódź, Poland

^b Foundry Research Institute, Zakopiańska 73, 30-418 Kraków, Poland

* Corresponding author. E-mail address: boguslaw.pisarek@p.lodz.pl

Received 06.04.2018; accepted in revised form 01.10.2018

Abstract

The article presents the investigations of 7xxx aluminium alloys performed by the method of thermal and derivational analysis. The studies made it possible to identify the effect of the changes in the Cu concentration, the total Zn and Mg weight concentrations and the Zn/Mg weight concentration ratio on their crystallization process: the cooling as well as the kinetics and dynamics of the thermal process of cooling and crystallization. Metallographic studies were performed on the microstructure of the examined alloys and their HB hardness was measured. The evaluation of the changes was presented in reference to the model alloys EN AW-7003 and EN AW-7010, whose microstructure under the conditions of thermodynamic equilibrium are described by the phase diagrams: Al-Zn-Mg and Al-Zn-Mg-Cu. The performed investigations confirmed that the hardness HB of the examined alloys is mainly determined by the reinforcement of the matrix α_{Al} by the introduced alloy additions and the presence of phases $\Theta(Al_2Cu)$ and $S(Al_2CuMg)$ rich in copper, as well as $\eta(MgZn_2)$, in the examined alloys' microstructure. The increase of the amount of intermetallic phases precipitated in the microstructure of the examined alloys is caused, beside Cu, by the characteristic change of Zn wt. concentration and Mg. It was proposed that the process of one-stage thermal treatment of the examined alloys be introduced at a temperature of up to $t_{j-20}^{\circ}C$, which will prevent the exceedance of the solidus temperature.

Keywords: Innovative Casting Materials and Technologies, Al-Zn-Mg-Cu Alloys, TDA Method, Microstructure, Hardness HB

1. Introduction

Aluminium alloys with zinc, magnesium and copper from the 7xxx series, with a properly applied thermal treatment, characterize in the highest strength properties of all the aluminium alloys [1]. The high properties of these alloys are provided by the copper and magnesium phases formed during the primary crystallization (directly in the liquid), which, during the thermal treatment, as a result of their decomposition, enable precipitation

hardening of the alloy's microstructure [2,3]. The crystallization process of these alloys is strongly affected by the change in the Zn, Mg and Cu concentration. In alloys of the Al-Zn-Mg-Cu system, beside the absolute content levels of the particular main alloy additions (Zn, Mg and Cu), such criterial quantities are also important as: the sum of the zinc and magnesium concentrations (Zn+Mg in % wt.) and the zinc and magnesium weight concentration ratio (Zn/Mg). The representative alloys from this series are: alloy EN AW-7003 (7003), whose microstructure, formed under phase equilibrium conditions, is described by the

diagram Al-Mg-Zn [4] and alloy EN AW-7010 (7010), whose microstructure, formed under phase equilibrium conditions, is described by the diagram Al-Zn-Mg-Cu [5]. We know little about the formation process of these alloys' microstructure evaluated by the method of thermal and derivational analysis (TDA). This method, under the conditions of the alloys' crystallization in a ceramic mould [6], cooling in ambient air, makes it possible to evaluate: the cooling $t=f(\tau)$, the change of kinetics $dt/d\tau=f'(\tau)$ and dynamics of the thermal crystallization processes $d^2t/d\tau^2=f''(\tau)$ in the function of the alloy's cooling time τ . The use of this method enables the determination of the characteristic temperature of phase transformations, confirming the formation of the expected phases or their systems in the microstructure, whose knowledge is necessary to determine the appropriate temperature of thermal treatment.

2. Work methodology

In order to examine the effect of a change in the concentration of the Zn and Mg additions in an aluminium alloy from the 7xxx series, according to PN-EN 573-3:2014-02 – English version, on the hardness HB, a two-level experiment schedule was elaborated by the Box-Wilson method, whose model has been shown in Figure 1 (a,b).

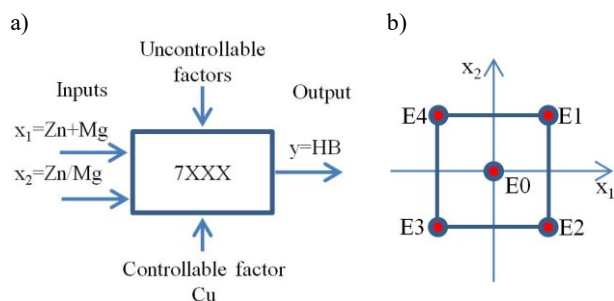


Fig. 1. General model of the system (a) and the Central Composite Design of Experiment (b)

As the input factors x_1 and x_2 the following were assumed: $x_1=Zn+Mg$ (% wt.) and $x_2=Zn/Mg$, and as the output factor – the alloy's hardness $y=HB$. As the constant value in the experiment, the concentration of $Cu \approx 0,75\%$ wt. was established. The values of the experiment settings E0–E4 are included in Table 1. The actual chemical compositions of the examined alloys are presented in Table 2. Additionally, three experiments were performed: E5 for alloy 7003, E6 for alloy 7010 and E7 for the alloy with the factor values of: $x_1 \approx 6$ and $x_2 \approx 2$.

The alloy was melted in the induction furnace Indutherm VC500 D, in a graphite crucible.

In order to identify the characteristic temperature of phase transformations and the duration time of the particular crystallization stages for the examined alloys, a thermal and derivational analysis was carried out in the ATD10PL tester (shell mould) [6]. Based on the recorded temperature of the alloy cooling in the TDA tester, the following characteristics were drawn: the cooling $t=f(\tau)$, the thermal process kinetics $dt/d\tau=f'(\tau)$ and the thermal process dynamics $d^2t/d\tau^2=f''(\tau)$.

The points determined on the characteristic curves describe: the phase transformation beginning, the maximal thermal effect or the end of the alloy's phase transformation taking place in the volume of the TDA tester.

Table 1.
Experimental design

	$x_1=Zn+Mg, \%$	$x_2=Zn/Mg, \%/ \%$
x_i^0 (E0)	6.5	3
Δx_i	1	1
$x_i^0 + \Delta x_i$	7.5	4
$x_i^0 - \Delta x_i$	5.5	2
E1	7.5	4
E2	7.5	3
E3	5.5	3
E4	5.5	4

Table 2.
Real chemical composition of researched alloys

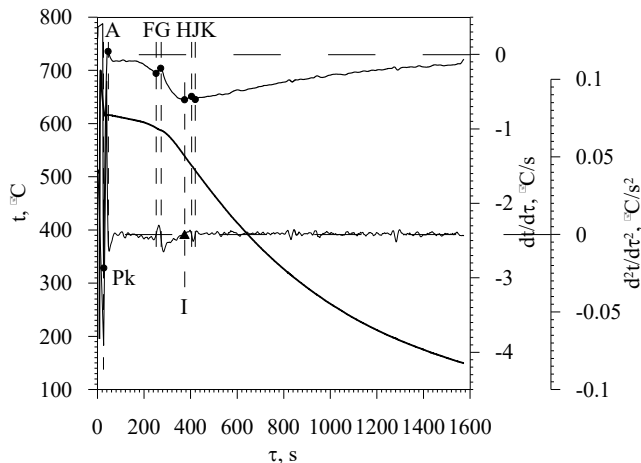
No probe	Chemical composition, wt. %					Zn+Mg, %	Zn/Mg, %/ %
	Al	Zn	Mg	Cu	Other		
E0	91.87	5.23	1.76	0.75	0.39	7.0	3.0
E1	90.72	6.90	1.14	0.75	0.49	8.0	6.1
E2	91.93	4.58	2.29	0.72	0.48	6.9	2.0
E3	93.72	3.85	1.30	0.75	0.38	5.2	3.0
E4	93.67	4.13	1.08	0.77	0.36	5.2	3.8
E5 (7003)	92.59	5.90	0.84	0.003	0.67	6.7	7.0
E6 (7010)	89.22	5.87	2.44	1.94	0.53	8.3	2.4
E7	92.91	4.06	1.88	0.76	0.39	5.9	2.2

The microstructure of the examined alloys after etching in a 10% HF solution in water was observed under a metallographic microscope with different magnifications. The alloys' hardness test was performed by the Brinell's method (steel ball $\varnothing 2.5$ mm, $k=10$).

3. Crystallization of alloys 7003 and 7010

The TDA characteristics for alloy E5 (7003) are presented in Figure 2. The crystallization of alloy E5 (7003) in the ATD10PL tester has a characteristic course. After the alloy's cooling below the equilibrium liquidus temperature, at the actual temperature $t_D=615,5$ °C, the primary phase α_{Al} ($L \rightarrow L + \alpha_{Al}$) nucleates and grows. The crystallization of phase α_{Al} does not fully exhaust the liquid L. The crystallization front of phase α_{Al} , mostly rich in aluminium, pushes the Zn and Mg atoms to the remainder of the uncrystallized liquid. Next, after the alloy's overcooling below the equilibrium temperature of the crystallization of the stable intermediate phase, at the temperature $t_G=587,4$ °C, a, probably non-equilibrium, phase of the $\eta(MgZn_2)$ ($L \rightarrow L + \eta(MgZn_2)$) type nucleates and grows. Under the thermodynamic equilibrium conditions in the Al-Mg-Zn system, this phase crystallizes at a temperature below 590 °C [4]. This stage of crystallization does not fully exhaust the liquid alloy, either. Next, after the alloy's overcooling below the equilibrium temperature of the peritectic

transformation at the temperature $t_J=521,4\text{ }^\circ\text{C}$, as a result of a peritectic reaction, a, probably non-equilibrium, phase of the $\tau_1(\text{Mg}_{32}(\text{Zn},\text{Al})_{48})$ ($\text{L}+\eta(\text{MgZn}_2)\rightarrow\tau_1(\text{Mg}_{32}(\text{Zn},\text{Al})_{48})$) type nucleates and grows. In the peritectic reaction, the liquid L is fully exhausted, yet phase $\eta(\text{MgZn}_2)$ is not, which is proved by the relatively small effect of this transformation H-J-K.



Points	τ, s	$t=f(\tau), \text{ }^\circ\text{C}$	$dt/d\tau=f'(\tau), \text{ }^\circ\text{C/s}$	$d^2t/d\tau^2=f''(\tau), \text{ }^\circ\text{C/s}^2 \times 10^{-3}$
Pk	26.9	626.4	-2.87	10.516
A	45.4	615.5	0.04	-0.048
F	251.5	591.8	-0.25	-0.032
G	271.4	587.4	-0.19	0.014
H	373.8	539.2	-0.61	-0.005
I	373.8	539.2	-0.61	-0.005
J	403.8	521.4	-0.56	0.004
K	419.8	512.1	-0.60	0.022

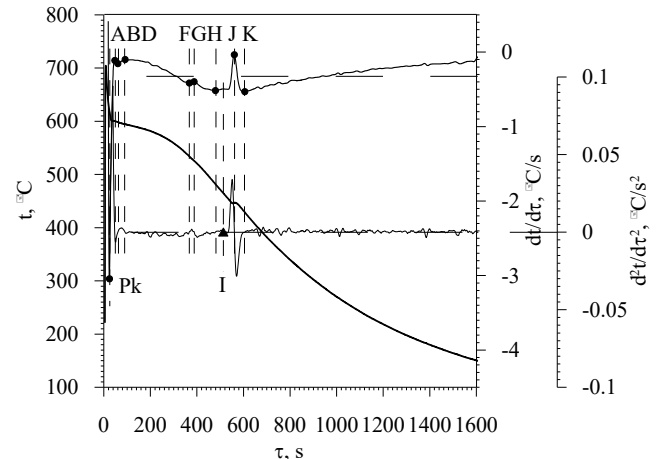
Fig. 2. TDA characteristics of alloy E5 (7003)

Under the conditions of thermodynamic equilibrium in the Al-Mg-Zn system, the peritectic reaction takes place at $530\text{ }^\circ\text{C}$ [4]. After the end of the peritectic transformation within the volume of the ATD10PL tester at the temperature $t_K=512,1\text{ }^\circ\text{C}$, alloy E5 (7003) cools down to the ambient temperature without the occurrence of phase transformations.

The TDA characteristics for alloy E6 (7010) have been shown in Figure 3. The crystallization process of alloy E6 (7010) in the ATD10PL tester has a characteristic course. After the alloy's overcooling below the equilibrium liquidus temperature at the actual temperature $t_A=600,6\text{ }^\circ\text{C}$, the primary phase α_{Al} ($\text{L}\rightarrow\text{L}+\alpha_{\text{Al}}$) nucleates and grows. The crystallization front of phase α_{Al} , mostly rich in aluminium, pushes the Zn, Mg and Cu atoms to the remainder of the uncrystallized liquid. Next, after the alloy's overcooling below the equilibrium temperature of the eutectic transformation at the temperature $t_D=594,3\text{ }^\circ\text{C}$, the, probably non-equilibrium, binary eutectic $\text{L}\rightarrow\text{L}+\text{eut.}(\alpha_{\text{Al}}+\Theta(\text{Al}_2\text{Cu}))$ nucleates and grows.

Under the conditions of thermodynamic equilibrium, the eutectic transformation in the Al-Cu-Mg system takes place at $<591\text{ }^\circ\text{C}$; a change in this value is also affected by the concentration of Zn in the alloy [5,7]. Next, after the alloy's

overcooling below the equilibrium temperature of the ternary eutectic's crystallization, the non-equilibrium eutectic $\text{L}\rightarrow\text{L}+\text{eut.}(\alpha_{\text{Al}}+\Theta(\text{Al}_2\text{Cu})+\text{S}(\text{Al}_2\text{CuMg}))$ nucleates and grows.



Points	τ, s	$t=f(\tau), \text{ }^\circ\text{C}$	$dt/d\tau=f'(\tau), \text{ }^\circ\text{C/s}$	$d^2t/d\tau^2=f''(\tau), \text{ }^\circ\text{C/s}^2 \times 10^{-3}$
Pk	24.3	620.1	-3.04	-3043.9
A	47.4	600.6	-0.11	-2.33
B	60.2	598.4	-0.15	-0.093
D	91.5	594.3	-0.1	-0.149
F	367.4	533.7	-0.41	0.034
G	387.8	525.6	-0.4	0.155
H	479.4	481.9	-0.52	-0.007
I	513.3	464.9	-0.5	0.039
J	560.6	446.4	-0.04	0.161
K	605.4	428.9	-0.53	-0.0004

Fig. 3. TDA characteristics of alloy E6 (7010)

Also in this case, the crystallization stage does not fully exhaust the liquid alloy. Next, after the alloy's overcooling below the equilibrium temperature of the crystallization of the stable intermediate phase, at $t_J=446,4\text{ }^\circ\text{C}$, a, probably non-equilibrium, phase of the $\eta(\text{MgZn}_2)$ ($\text{L}\rightarrow\eta(\text{MgZn}_2)$) type nucleates and grows from the remainder of the unsolidified alloy. Under the conditions of thermodynamic equilibrium in the Al-Mg-Zn system, this phase crystallizes at a temperature below $590\text{ }^\circ\text{C}$ [3].

After the end of the crystallization of phase $\eta(\text{MgZn}_2)$ within the volume of the ATD10PL tester at $t_K=428,9\text{ }^\circ\text{C}$, alloy E6 (7010) cools down to the ambient temperature without the occurrence of phase transformations.

The microstructure of alloys E5 (7003) and E6 (7010) has been presented in Figures 4 and 5, respectively. The microstructure of alloy E5 (7003) is probably composed of phases of the following types: α_{Al} , $\eta(\text{MgZn}_2)$, as well as the peritectic phase $\tau_1(\text{Mg}_{32}(\text{Zn},\text{Al})_{48})$. The microstructure of alloy E6 (7010) is probably composed of the following types of phases: α_{Al} , binary eutectic $(\alpha_{\text{Al}}+\Theta(\text{Al}_2\text{Cu}))$, ternary eutectic $(\alpha_{\text{Al}}+\Theta(\text{Al}_2\text{Cu})+\text{S}(\text{Al}_2\text{CuMg}))$ and $\eta(\text{MgZn}_2)$.

A change in the Zn, Mg and Cu concentration in the examined alloys affects mostly crystallization similar to that of alloy E5 (7003), which solidifies according to the phase equilibrium

system Al-Zn-Mg, or that of E6 (7010), solidifying according to the equilibrium system Al-Zn-Mg-Cu (Tab. 2). Alloys E5 (7003) and E4 have similar courses of TDA characteristics as well as similar microstructures. Despite the presence of about 0.77% Cu in alloy E4, on the TDA characteristics it is difficult to determine the thermal effect from the copper phase crystallization, and in the microstructure of this alloy, no areas of $\alpha_{Al}+\Theta(Al_2Cu)$ type eutectic were observed. And so, at this stage of research, an assumption was made of a higher probability of this alloy's crystallization into alloy E5 (7003) than into alloy E6 (7010). In turn, alloys E0, E2, E3 and E7 have similar courses of ATD characteristics as well as similar microstructures to those of alloy E6 (7010). A change in the concentration of the examined additions mostly affects the percentage of the crystallized phases or phase systems (e.g. eutectics).

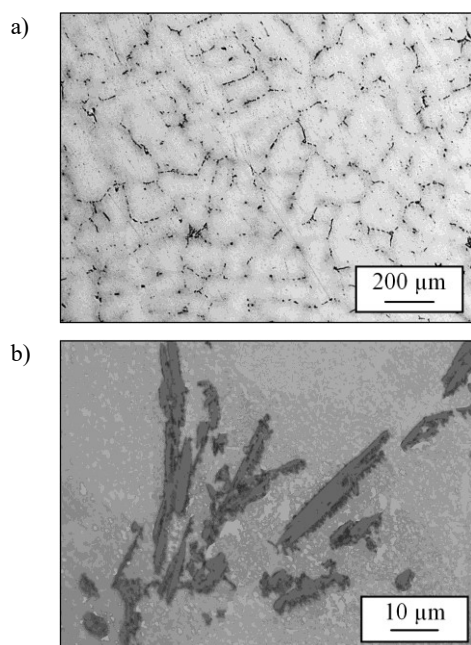


Fig. 4. Microstructure (a, b) of alloy E5 (7003): $\alpha_{Al}+\eta(MgZn_2)+\tau_1(Mg_{32}(Zn,Al)_{48})$

The measurements of hardness HB in the as-cast state of the examined alloys are presented in Table 3.

The evaluation of the effect of a change in the Zn and Mg concentration in the form of the relation Zn+Mg, Zn/Mg and Cu on the crystallization process (characteristic temperatures of maximal thermal effects) and hardness HB for the performed experiments (Tab. 1) have been presented in Figures 6–9, for:

- Zn+Mg \approx 5; effect of the change in the Zn/Mg ratio on the temperature of characteristic phase transformations and hardness HB of alloys E4 and E3 (Fig. 6),
- Zn+Mg \approx 6; and the Zn/Mg \approx 2 ratio on the temperature of characteristic phase transformations and hardness HB of alloy E7 (Fig. 7),
- Zn+Mg \approx 7; effect of the change in the Zn/Mg ratio on the temperature of characteristic phase transformations and hardness HB of alloys E0, E2 and E5 (Fig. 8),

- Zn+Mg \approx 8; effect of the change in the Zn/Mg ratio on the temperature of characteristic phase transformations and hardness HB of alloys E1 and E6 (Fig. 9).

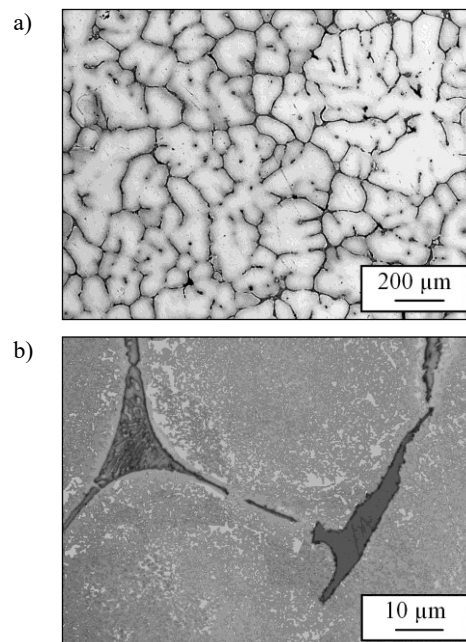


Fig. 5. Microstructure (a, b) of alloy E6 (7010): $\alpha_{Al}+\Theta(Al_2Cu)+S(Al_2CuMg)+\eta(MgZn_2)$

The crystallization of alloy E5 (7003) includes three stages of primary crystallization (Fig. 2):

- Pk-A-F – crystallization of phase α_{Al} ,
- F-G-H – crystallization of $\eta(MgZn_2)$ type phase,
- H-I-J-K – crystallization of $\tau_1(Mg_{32}(Zn,Al)_{48})$ type phase.

Table 3. Hardness HB tests, mean hardness HB_m and standard deviation σ for the tested aluminium alloys

No probe	1	2	3	4	5	6	HB_m	σ
E0	98.3	95.6	101.0	97.4	99.7	98.8	98.5	1.87
E1	113.0	108.0	110.0	114.0	113.0	113.0	111.8	2.32
E2	99.5	97.9	97.9	93.7	98.1	99.0	97.7	2.06
E3	90.5	91.5	94.0	94.0	93.2	95.8	93.2	1.91
E4	88.3	88.5	89.9	82.0	87.1	89.1	87.5	2.84
E5 (7003)	89.2	84.7	84.2	88.6	85.4	90.8	87.2	2.73
E6 (7010)	114.0	112.0	115.0	109.0	115.0	114.0	113.2	2.32
E7	91.1	91.1	91.1	92.0	92.8	89.9	91.3	0.98

Conditions for HB hardness optimization (if Cu=const.): direction E0–E1 (maximization HB) – $x_1\uparrow$ (Zn \uparrow , Mg \uparrow) and $x_2\uparrow$ (Zn \uparrow , Mg \downarrow), therefore Mg=const. and Zn \uparrow ; direction E0–E4 (minimization HB) – $x_1\downarrow$ (Zn \downarrow , Mg \downarrow) and $x_2\uparrow$ (Zn \uparrow , Mg \downarrow), therefore Zn=const. and Mg \downarrow .

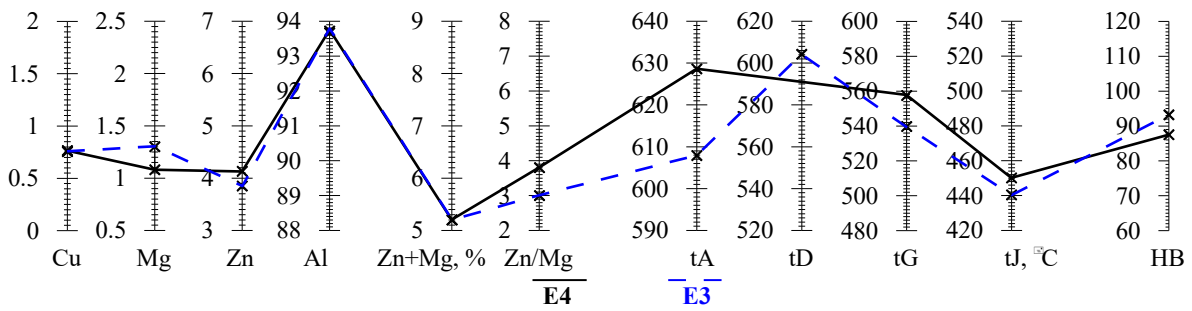


Fig. 6. Effect of the change in the Zn/Mg chemical composition ratio for Zn+Mg≈5% on the temperature of characteristic phase transformations of alloys E4 and E3 and their hardness HB

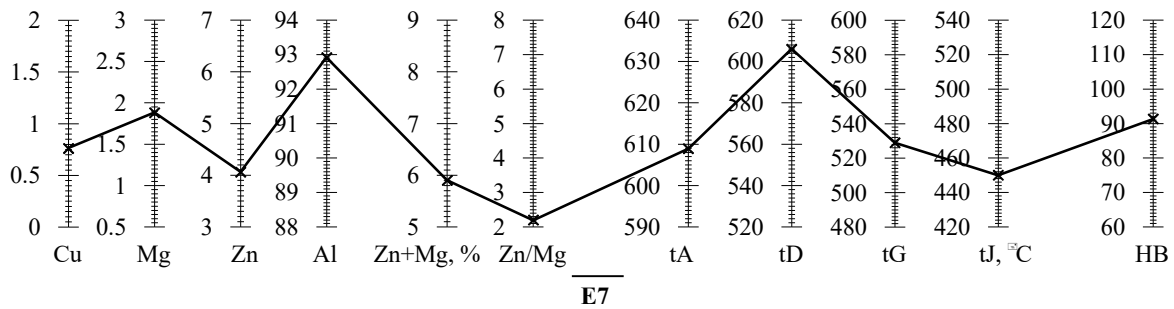


Fig. 7. Effect of the change in the Zn/Mg chemical composition ratio for Zn+Mg≈6% on the temperature of characteristic phase transformations of alloy E7 and hardness HB

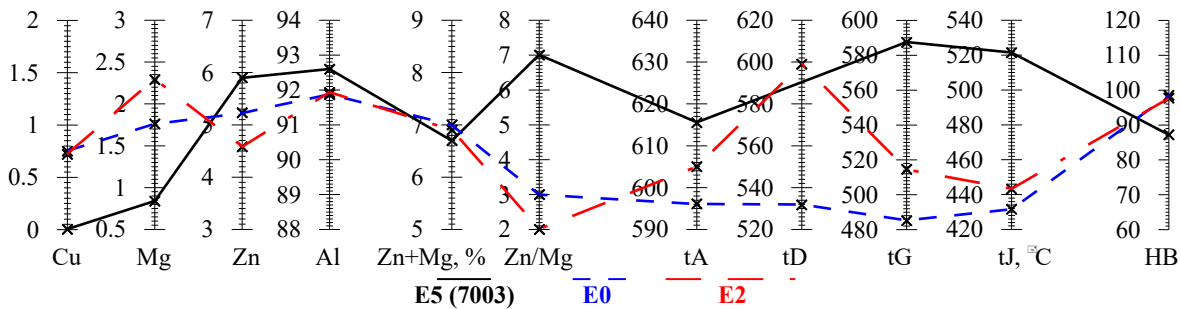


Fig. 8. Effect of the change in the Zn/Mg chemical composition ratio for Zn+Mg≈7% on the temperature of characteristic phase transformations of alloys E5 (7003), E0 and E2 and their hardness HB

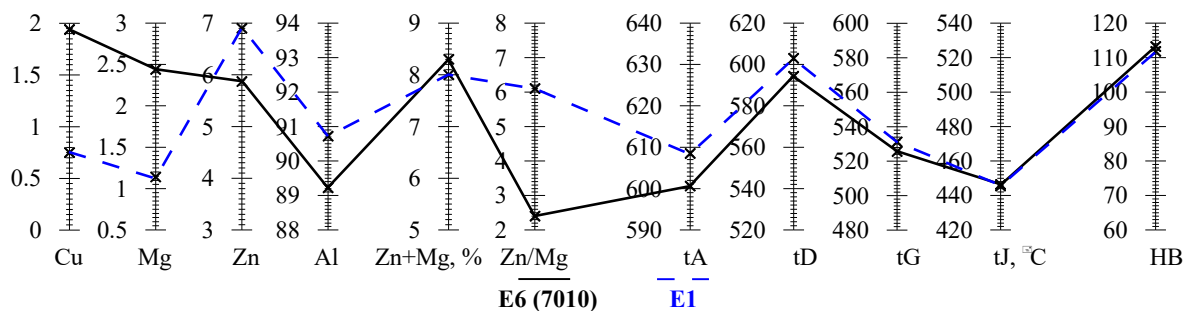


Fig. 9. Effect of the change in the Zn/Mg chemical composition ratio for Zn+Mg≈8% on the temperature of characteristic phase transformations of alloys E6 (7010) and E1 and their hardness HB

The process of primary crystallization of the examined alloy in the TDA tester ends at a relatively high temperature, $t_K=521.4\text{ }^\circ\text{C}$ and after a short time, $\tau_K-\tau_{Pk}=392.9\text{ s}$. Alloy E5 (7003) cast into the TDA tester characterizes in hardness at the level of 87.2 ± 1.73

HB (Tab. 3). In turn, compared to alloy E5 (7003), alloy E6 (7010), with a higher content of Mg, i.e. about 1.5%, and about 2% Cu, characterizes in a larger number of stages (4 stages) of primary crystallization (Fig. 3):

- Pk-A-B – crystallization of phase α_{Al} ,
- B-D-F – crystallization of $\alpha_{Al}+\Theta(Al_2Cu)$ type binary eutectic,
- F-G-H – crystallization of $\alpha_{Al}+\Theta(Al_2Cu)+S(Al_2CuMg)$ type ternary eutectic,
- I-J-K – crystallization of $\eta(MgZn_2)$ type phase.

In consequence of this multi-stage crystallization process, as a result of a change in the chemical composition of the alloy (compared to alloy E5 (7003)), the alloy ends its primary crystallization at a temperature about 82 °C lower, i.e. $t_K=428,9$ °C. This causes a prolongation of the time of primary crystallization by about 188 s ($\tau_K-\tau_{Pk}=581,1$ s). Alloy E6 (7010) cast into the TDA tester, compared to alloy E5 (7003), characterizes in hardness at the level of $113,2\pm 2,32$ HB (Tab. 3, Fig. 8 and Fig. 9). The hardness increase is caused mostly by the $\Theta(Al_2Cu)$ and $S(Al_2CuMg)$ type phase formed in the alloy's microstructure. For the examined alloys, the actual liquidus temperature of the primary crystallization of phase α_{Al} t_A is within the scope of 596.1–628.6 °C. For the alloys containing a Cu addition in the scope of 0.75–1.94% wt., the actual crystallization temperature t_D of the $\alpha_{Al}+\Theta(Al_2Cu)$ type binary eutectic is within the scope of 531.7–605.9 °C, and that of the crystallization of the $\alpha_{Al}+\Theta(Al_2Cu)+S(Al_2CuMg)$ type ternary eutectic, t_G is within the scope of 485.1–539.1 °C. For the examined alloys, the actual crystallization temperature t_J of the $\eta(MgZn_2)$ type phase is within the scope of 431.6–450.0 °C, whereas for alloy E5 (7003), which contains no Cu addition, t_G equals 587.4 °C. While designing the thermal treatment of these alloys, one should assume that the maximal temperature should not exceed the alloy's solidus temperature. And so, based on the obtained temperate measurements, it is estimated that the maximal temperature of this process should not be higher than t_J-20 °C. It is possible to apply a multi-stage thermal treatment and anneal the alloy gradually, enabling a diffusive dissolution of phases η , Θ and S in the matrix, thus avoiding their melting. It can be inferred from the conducted investigations that the hard-ness of alloy E5 (7003) is mostly determined by: phase α_{Al} reinforced with Zn and Mg, and intermetallic precipitations of the $\eta(MgZn_2)$ type phase. In the case of the remaining alloys containing a Cu addition, which, similarly to Zn and Mg, also hardens the precipitations of the primary phase α_{Al} , their hardness, beside the $\eta(MgZn_2)$ type phase, is also determined by the $\Theta(Al_2Cu)$ and $S(Al_2CuMg)$ type phases rich in Cu. In the analysis (Fig. 6 – Fig. 9) of the effect of a change in the total content of Zn and Mg ($x_1=Zn+Mg$) in the alloy and the concentration wt. ratio of Zn and Mg ($x_2=Zn/Mg$) contained in it, it was found that with increasing Zn wt. concentration (at constant Mg wt. concentration) the HB hardness of the alloy increases, whereas the decrease in Mg wt. concentration (at constant Zn wt. concentration) reduces the HB hardness of the alloy.

4. Conclusions

The performed research makes it possible to draw the following conclusions:

- The crystallizations and microstructures of the following alloys are similar:
 - E4 to E5 (7003),

- E0–E3 and E7 to E6 (7010),
- The hardness of the examined alloys in the as-cast state is within the scope between that of alloy E5 (7003) 87 HB, and that of alloy E6 (7010) 113 HB,
- The increase of the examined alloys' hardness is mostly affected by the Cu addition, which hardens the matrix α_{Al} and forms intermetallic phases Θ and S ,
- From the analysis of the effect of a change in the sum of Zn+Mg concentrations wt. in the alloy and the Zn/Mg concentration wt. ratio, it can be concluded that Zn increases the alloy's hardness more significantly than Mg, by reinforcing the matrix α_{Al} and forming intermetallic phases η ,
- The one-stage process of thermal treatment of the examined alloys should be carried out at a temperature not higher than t_J-20 °C.

References

- [1] PN-EN 573-3:2014-02 - English Version - Aluminium and aluminium alloys - Chemical composition and form of wrought products - Part 3: Chemical composition and form of products.
- [2] Górny, Z., Sobczak, J. (2005). Modern materials molding on the basis of non-ferrous metals. Kraków: ZA-PIS. (in Polish)
- [3] Ghosh, A. & Ghosh, M. (2018). Microstructure and texture development of 7075 alloy during homogenisation, *Philosophical Magazine*. 1-21. DOI: 10.1080/14786435.2018.1439596.
- [4] Petrov, D., Watson, A., Gröbner, J., Rogl, P., Tedenac, J.-C., Bulanova, M., Turkevich, V. & Lukas, H.L. (2005). Al-Mg-Zn (Aluminium - Magnesium - Zinc). In Effenberg G. & Ilyenko S. (Eds.). Landolt-Börnstein - Group IV Physical Chemistry 11 A3, Light Metal Systems. Part 3. Retrieved February 16, 2018, from SpringerMaterials. https://materials.springer.com/lb/docs/sm_lbs_978-3-540-31694-7_21. DOI: 10.1007/10915998_21.
- [5] Akopân, T.K., Zolotarevskij, V.S. & Hvan, A.V. (2013). Rasčet Fazovyh Diagramm Sistem Al-Cu-Zn-Mg i Al-Cu-Zn-Mg-Fe-Si. *Litejnoe proizvodstvo*. 3, 44-51. (in Russian).
- [6] Rapijko, C., Pisarek, B., Czekaj, E. & Pacyniak, T. (2014). Analysis of AM60 and AZ91 alloy crystallisation in ceramic moulds by Thermal Derivative Analysis (TDA). *Archives of Metallurgy and Materials*. 59(4), 1449-1455. DOI: 10.2478/amm-2014-0246.
- [7] Effenberg, G., Prince, A., Lebrun, N., Lukas, H. & Harmelin, M. (2004). Al-Cu-Mg (Aluminium - Copper - Magnesium). In Effenberg G. & Ilyenko S. (Eds.). Landolt-Börnstein - Group IV Physical Chemistry 11 A2, Light Metal Systems. Part 2. Retrieved February 16, 2018, from SpringerMaterials. https://materials.springer.com/lb/docs/sm_lbs_978-3-540-31687-9_4. DOI: 10.1007/10915967_4.